A Limit to TDC Turbulence Intensity in Internal Combustion Engines

M.E. Hayder,* A.K. Varma,† and F.V. Bracco‡
Princeton University, Princeton, New Jersey

The turbulence level near top dead center (TDC) in an internal combustion engine strongly influences the flame propagation and the combustion processes. The effect of intake system design on TDC turbulence has recently been studied experimentally. This paper presents comparisons of the predictions of a model for the turbulent flowfields with those experimental data taken in a ported engine with and without swirl and in a valved engine without swirl. The model is for an axisymmetric geometry and uses a k-ϵ submodel for turbulent transport. The model constants are the same as those used in several previous studies. The computed results show fairly good agreement with the measurements. The two-dimensional results are also compared with those from a zero-dimensional model and serious limitations of the zero-dimensional model are evidenced. The two-dimensional calculations lead to the important conclusion that there is an upper limit to the magnitude of the TDC turbulence intensity in reciprocating engines with pancake combustion chambers. This limit is independent of the characteristics of the flowfield at the end of the intake processes and is due to the chamber walls. Below the limit, TDC turbulence intensity is influenced primarily by the turbulent diffusivity of the gas at the end of the intake process.

Nomenclature

A = chamber cross-sectional area
A_i = intake area
C_μ, C_1, C_2, C_3 = constants in the turbulence model
CL = TDC clearance, cm
D = effective diffusivity, cm^2/s
k = kinetic energy of turbulence, cm^2/s^2
ℓ = turbulence scale, $-C_\mu^{3/4} k^{3/4}/\epsilon$
h = distance between piston and cylinder head; also an engine length scale
p = pressure, dynes/cm^2
r,z = coordinate directions, cm
R = half bore of cylinder, cm
t = time, s
T = temperature, K
u_r = component of velocity in r direction, cm/s
u_z = component of velocity in z direction, cm/s
$\boldsymbol{u}$ = velocity vector
U_p = piston velocity, cm/s
w = component of velocity in tangential direction, cm/s
α,β = dimensional constants that determine initial values of k and ϵ
ϵ = dissipation rate of turbulence kinetic energy, cm^2/s^3
η_v = volumetric efficiency
θ = crankangle
θ_i = crankangle of intake opening, radians
κ = model constant (0.84)
μ = effective viscosity, g/cm·s
ν = kinematic viscosity, cm^2/s
ρ = density, g/cm^3
$\sigma_k, \sigma_\epsilon$ = diffusion model constants in k and ϵ equations
ϕ = dimensionless time scale $\epsilon/k\omega_0$
χ,ψ = dimensionless contents that determine initial values of k and ϵ
ω_0 = angular velocity of engine

Subscripts

0 = initial values
TDC = value of top dead center
T = turbulent

Superscripts

T = transpose
$(\bar{\ })$ = average value
$(\ )'$ = fluctuating component

Received July 11, 1984; revision received March 5, 1985.

*Graduate Student, Department of Mechanical and Aerospace Engineering.
†Research Staff Member, Department of Mechanical and Aerospace Engineering.
‡Professor, Department of Mechanical and Aerospace Engineering.

I. Introduction

THE velocity field in an internal combustion (IC) engine is turbulent and nonstationary. The turbulence levels are important because of their effect on the flame speed and, thereby, the combustion rate and the efficiency of the engine. The relationship between engine turbulence and the geometrical parameters and operating conditions of an engine has been studied by many researchers.[1-10] Experimentally, due to the difficulty of making turbulence measurements in combusting flows, this dependence has typically been investigated under motored nonfiring conditions. Although it is possible that the combustion process itself may effect turbulence, cold-flow studies are still useful as indicators of the properties of engine turbulence and provide a data base for the development of models of the engine flowfields.

Measurements of engine turbulence have been made both with hot-wire anemometry[1,2,11] and laser Doppler velocimetry (LDV).[10,12,13] The data of Lancaster[2] and Johnston et al.[12] have previously been used in the numerical modeling studies of Grasso and Bracco.[9] They used an unsteady axisymmetric model with a k-ϵ turbulence submodel to explore the effect of various aspects of chamber design and engine operating conditions on top dead center (TDC) turbulence and showed good agreement with the experimental data. The same model is used in the present study. The original focus of the study was to compare the model predictions to the recent extensive cycle-resolved measurements of near-TDC turbulence in motored, ported, and valved IC engines using LDV[10,14,15] at practical

engine speeds. However, the study broadened into an investigation of the sources and sinks of turbulence during compression and of the sensitivity of the TDC flowfield to initial conditions, engine geometry, and model constants. This led to the realization that there are limits to the intensity of the turbulence that can be achieved in a simple pancake combustion chamber near TDC, that is, at the time combustion occurs in an IC engine.

The next section briefly describes the model and a more general formulation of the initial conditions than that used by Grasso and Bracco.[9] Section III discusses certain simplified solutions of the k-ϵ equations that are obtained under restricted conditions. Section IV describes the results obtained from the complete model including comparisons with the simplified solutions, a sensitivity study with respect to model constants, and comparisons with the new[14,15] measurements of TDC turbulence intensity in a ported engine with and without swirl and in a valved engine without swirl. Conclusions are summarized in Sec. V.

II. Model

The governing equations and boundary conditions are detailed in Grasso and Bracco[9] and are not repeated here. The model is for the fluid motion in a two-dimensional axisymmetric engine. Conservation equations for the mean mass, momentum, and energy are solved numerically along with equations for the turbulence kinetic energy k and its dissipation rate ϵ. Bulk viscosity and body forces are neglected and the effective Prandtl and Schmidt numbers are assumed to be unity. The model constants in the equations are kept unchanged from our previous studies,[9] but we also carried out a sensitivity study on the values of these constants.[16]

The initial conditions were specified as follows. Computations for the sensitivity tests for the ported engine were started from -160 deg (160 deg before top dead center). All other computations were started at the midpoint of the intake opening with all of the initial mean velocities set equal to zero except for those problems involving swirl (axis of bulk motion coinciding with engine axis) or roll (axis of bulk motion normal to engine axis) motions. The thermodynamic variables ρ, p, and T were calculated assuming isentropic changes between the end of the intake and the crankangle at the beginning of the computations.

The initial values of the turbulence kinetic energy and its dissipation rate were related by Grasso and Bracco[9] to the engine rpm and the volumetric efficiency (load) through the intake velocity. They proposed the following expressions:

$$k=\alpha\eta_v^2\text{rpm}^2$$

$$\epsilon=\beta\eta_v^3\text{rpm}^3 \tag{1}$$

where α and β are dimensional empirical constants.

Again assuming that the initial turbulence intensity is proportional to a characteristic intake velocity and introducing an explicit initial reference length scale $A_i^{1/2}$, Eq. (1) can be rewritten as follows for the volumetric efficiency of 100% that is of interest in the current studies:

$$k=\chi\left(\frac{A}{A_i}\right)^2\frac{1}{\theta_i^2}\bar{U}_p^2$$

$$\epsilon=\psi\left(\frac{A}{A_i}\right)^3\frac{1}{\theta_i^3}\frac{1}{\sqrt{A_i}}\bar{U}_p^3 \tag{2}$$

where χ and ψ are dimensionless constants; A and A_i the piston and miximum open intake areas, respectively; θ_i the intake angle in radians; and $\bar{U}_p$ the mean piston speed. For a given engine, the constants χ and ψ are uniquely related to α and β. But χ and ψ should be valid for classes of engines, even though their values are still to be determined by comparison with the measurements. In our study, we will first make them compatible with the values of α and β and then show the sensitivity of the results to changes in their values. Grasso and Bracco[9] found that the initial diffusivity parameter α^2/β was mainly important in determining the TDC turbulence intensity in pancake chamber geometries. The corresponding parameter is now χ^2/ψ and its effect on the results will be discussed.

Figure 1 presents a sketch of the ported and valved engines showing the intake geometries and lists the important characteristics of the two engines.

III. Solutions of the k-ϵ Equations for Pure Compression without Wall Shear

With certain simplifying assumptions, it is possible to obtain analytic solutions of the k-ϵ equations. These solutions are useful in elucidating the effects of some of the parameters on the turbulence intensity during compression. However, as will be shown, in many practical cases the effects neglected become important and lead to significantly different results.

The primary simplifying assumption is the neglect of the diffusion terms in the k and ϵ equations, thus assuming a homogeneous turbulence field and disregarding all wall effects except bulk compression. Indeed, the order of magnitude of the diffusion terms compared to the turbulent dissipation terms is ℓ^2/L^2, where $\ell=C_\mu^{3/4}k^{3/2}/\epsilon$ is the turbulence length scale and L the chamber radius for radial diffusion or half the distance between the piston and the cylinder head for axial diffusion. If $\ell^2/L^2\ll 1$, the diffusion terms in the k and ϵ equations can be neglected. We consider a unidirectional axial compression process similar to that considered by Morel and Mansour,[8] although there are significant differences from their analysis. Other related studies have been reported by Borgnakke et al.,[17] Tabaczynski, [18] Reynolds,[19] and Davis et al.[20] The complete production term P^k is

$$P^k=\nu_T[\nabla u+\nabla u^T]:\nabla u-\frac{2}{3}\nabla\cdot u[k+\nu_T\nabla\cdot u] \tag{3}$$

Under the above assumptions, P^k simplifies to

$$P^k=-\frac{2}{3}k\nabla\cdot u+\frac{4}{3}\nu_T(\nabla\cdot u)^2 \tag{4}$$

$$\nabla\cdot u=\frac{U_p}{L}=\frac{1}{L}\frac{dL}{dt} \tag{5}$$

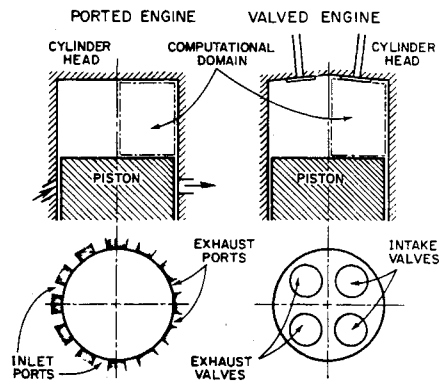

	PORTED 2 STROKE	VALVED 4 STROKE
BORE (cm)	8.26	8.26
STROKE (cm)	11.43	11.43
COMPRESSION RATIO	13.5	8.5
CLEARANCE (cm)	0.68	1.92
INTAKE AREA (cm²)	5.8	13.8
INTAKE (deg, TDC=0)	±126	−4, +222
EXHAUST (deg, TDC=0)	±113	+136, +4

Fig. 1 Sketches and characteristics of the ported and valved engines showing the intake configuration and the computational domain.

where U_p is the instantaneous piston velocity and L the distance between the piston and cylinder head. The k-ϵ equations become

$$\frac{dk}{dt} = P^k - \epsilon \tag{6}$$

$$\frac{d\epsilon}{dt} = C_1 P^k \frac{\epsilon}{k} + C_3 (\nabla \cdot u)\epsilon - C_2 \frac{\epsilon^2}{k} \tag{7}$$

Defining a dimensionless time scale $\phi = \epsilon/k\omega_0$, where $\omega_0 = \pi(\text{rpm})/30$ is the engine angular velocity, and using Eq. (5), the k and ϵ equations for an unsteady zero-dimensional model become

$$\frac{dk}{d\theta} = k\left[-\frac{2}{3}\frac{1}{L}\frac{dL}{d\theta} + \frac{4}{3\phi}C_\mu\left(\frac{1}{L}\frac{dL}{d\theta}\right)^2 - \phi\right] \tag{8}$$

$$\frac{d\epsilon}{d\theta} = \epsilon\left[\left(-\frac{2}{3}C_1 + C_3\right)\frac{1}{L}\frac{dL}{d\theta} + \frac{4}{3\phi}C_1 C_\mu\left(\frac{1}{L}\frac{dL}{d\theta}\right)^2 - C_2\phi\right] \tag{9}$$

These equations are solved numerically and the calculated results for $u' = (2/3k)^{1/2}$ and $\ell = C_\mu^{3/4}k^{3/2}/\epsilon$ are shown in Figs. 2 and 3. Morel and Mansour[8] used the same production term, but neglected the turbulent dissipation ϵ, which will be shown to be important during compression. The figures also show the results for an even simpler case in which the production term P^k is taken to be just $-2/3k\nabla \cdot u$. This is the correct production term if the turbulent stress tensor $\overline{u_i' u_j'}$ is isotropic, that is, if modeled as $\overline{u_i' u_j'} = 2k/3\delta_{ij}$. This approximation is also justified later when all components of P^k are examined in the numerical solution of the two-dimensional model and the term $2/3k\nabla \cdot u$ is normally found to be significantly larger than $\nu_T(\nabla \cdot u)$. Then Eqs. (8) and (9) become

$$\frac{dk}{d\theta} = k\left[-\frac{2}{3}\frac{1}{L}\frac{dL}{d\theta} - \phi\right] \tag{8a}$$

$$\frac{d\epsilon}{d\theta} = \epsilon\left[\left(-\frac{2}{3}C_1 + C_3\right)\frac{1}{L}\frac{dL}{d\theta} - C_2\phi\right] \tag{9a}$$

These equations are solved analytically to yield

$$k = k_0\left(\frac{L_0}{L}\right)^{2/3}\left[1 + \frac{\epsilon_0}{k_0\omega_0}(C_2 - 1) \times \int_{\theta_0}^{\theta}\left(\frac{L}{L_0}\right)^{C_3 + 2/3(1-C_1)} d\theta\right]^{-1/(C_2-1)} \tag{10}$$

The integral in the above expression can be calculated for a particular engine for any specified θ_0 and final θ. Using the parameters of the ported IC engine of Fig. 1, if $k_0 = 6 \times 10^4$ cm^2/s^2 ($u_0' = 200$ cm/s) and $\chi^2/\psi \sim 0.2$, then the second term within the brackets is ~ 2.0. For smaller values of χ^2/ψ, this second term becomes proportionally larger and 1 can be neglected in comparison. Then, approximating $C_2 - 1 \approx 1$, the expression becomes

$$k \approx \frac{k_0^2}{\epsilon_0}\left(\frac{L_0}{L}\right)^{2/3}\omega_0\left[\int_{\theta_0}^{\theta}\left(\frac{L_0}{L}\right)^{C_3 + 2/3(1-C_1)} d\theta\right]^{-1}$$

$$\text{for} \quad \chi^2/\psi \ll 0.2 \tag{11}$$

That is, k at TDC varies directly with the initial turbulent diffusivity $D_0 = C_\mu k_0^2/\epsilon_0$ for a given engine design and speed.

For larger values of χ^2/ψ, the second term of Eq. (10) becomes smaller than 1 and this simplified analysis for isotropic turbulence predicts that the final k depends only on k_0,

$$k \simeq k_0(L_0/L)^{2/3} \quad \text{for} \quad \chi^2/\psi \gg 0.2 \tag{12}$$

The factor L_0/L in all the above expressions brings in the effect of compressibility on k. For incompressible flow, the solution for k has the form

$$k = k_0\left[1 + \frac{\epsilon_0}{k_0}(C_2 - 1)t\right]^{-1/(C_2-1)} \tag{13}$$

For incompressible flow, turbulence always decays in the absence of mean shear. The results for incompressible flow are also shown in Fig. 2 for the same four values of χ^2/ψ. Production due to compression causes an increase in u' during the compression stroke. In the expansion stroke, the divergence of velocity that changes sign at TDC results in a steeper decay of u' than in incompressible cases. The term $(L_0/L)^{2/3}$ in Eq. (10) tends to increase (decrease) k during the compression (expansion) stroke, while the integral term is always positive and tends monotonically to decrease k. The relative importance of these two effects is determined by the ratio of the initial time scales $\epsilon_0/k_0\omega_0$. Near TDC, as the piston slows down, the change in L_0/L is small and turbulent dissipation dominates over the compression production and u' starts decreasing before the piston reaches TDC. For lower values of χ^2/ψ (or k_0^2/ϵ_0), the decay term is larger and the peak u' shifts away from TDC as shown in Fig. 2. The corresponding behavior of the turbulence length scale ℓ is shown in Fig. 3. The length scale for $\chi^2/\psi = 20.0$ is unreasonably large compared to the engine dimensions and this case should be considered only as a numerical experiment.

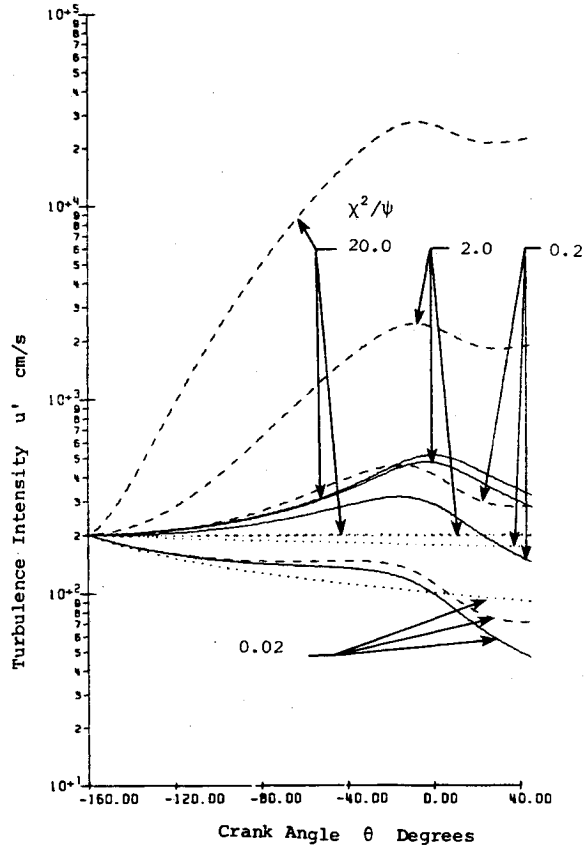

Fig. 2 Variation of turbulence intensity with crankangle predicted by the zero-dimensional model for different values of the diffusivity parameter χ^2/ψ: · · · · incompressible results, —— compressible results for $P^k = -2/3\ k\nabla \cdot u$, ---- compressible results for $P^k = -2/3\ k\nabla \cdot u + 4/3\ (\nu_T\ \nabla \cdot u)^2$ (ported engine, rpm = 2400).

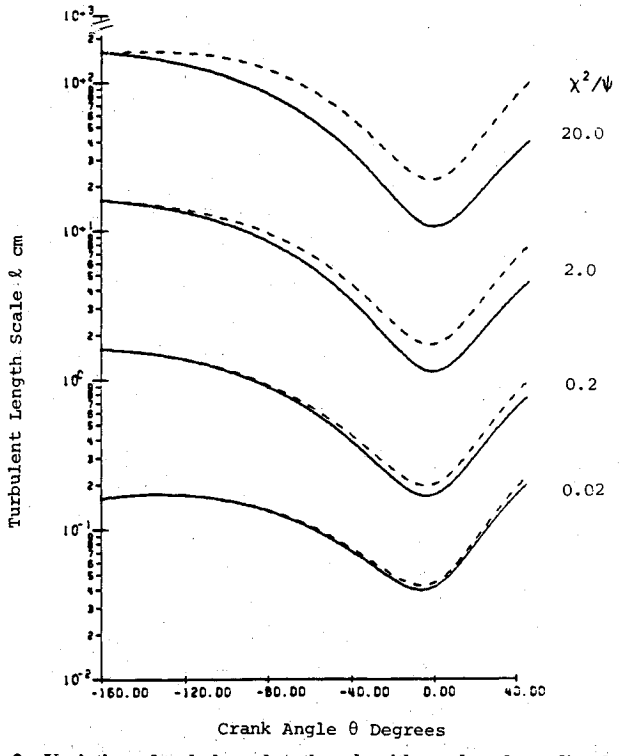

Fig. 3 Variation of turbulence length scale with crankangle predicted by the zero-dimensional model for different values of the diffusivity parameter χ^2/ψ: —— compressible results for $P^k = -2/3\ k\nabla\cdot u$, ---- compressible results for $P^k = -2/3\ k\nabla\cdot u + 4/3\ \nu_T\ (\nabla\cdot u)^2$ (ported engine, rpm = 2400).

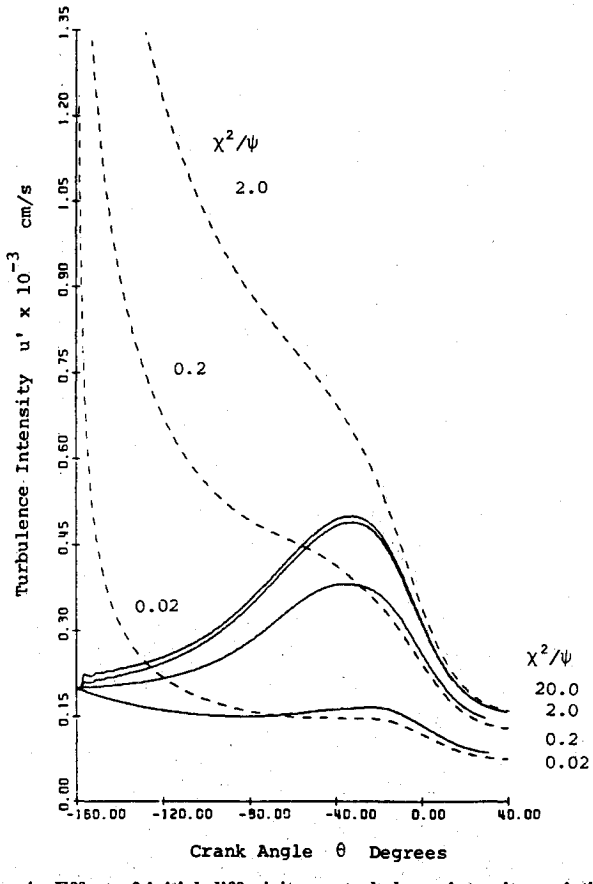

Fig. 4 Effect of initial diffusivity on turbulence intensity variation with crankangle: —— $u_0' = 200$ cm/s, ---- $u_0' = 2000$ cm/s (two-dimensional model, ported engine, rpm = 2400, $\bar{U}_p = 914$ cm/s).

These length scale results will be compared later to those obtained from the complete model, so discussion is deferred to that point. In the solutions with P^k given by Eq. (3), the surprising feature is the substantially higher values of u' obtained for the larger values of χ^2/ψ, when the $[4/3\nu_T(\nabla\cdot u)^2]$ term is added to the production term P^k in these simplified solutions. It was pointed out earlier that this term is much smaller than $(-2/3k\nabla\cdot u)$ for the full solution of the partial differential equations in the engine chamber. However, in the simplified solution, the chamber walls are ignored (that is, the wall boundary conditions on k and ϵ are not used) and this leads to substantially smaller values of ϵ in the simplified solutions than in the complete solution. This increases the relative magnitude of the $[4/3\nu_T(\nabla\cdot u)^2]$ part of P^k and leads to the higher u' values seen in Fig. 2. This is an example of the serious deficiencies that can limit the usefulness of the simplified analyses.

IV. Model Results and Sensitivity to Various Parameters

The results obtained from the numerical solution of the full set of two-dimensional model equations will now be considered. The results will be compared to the measurements of Liou et al.[10,14,15] in ported and valved IC engines. The sensitivity of the results to initial conditions, various model parameters, and engine flowfields will be discussed.

Effect of Initial Diffusivity and Initial Turbulence Level

Grasso and Bracco[9] reported that the initial diffusivity

$$D_0 = C_\mu \frac{k_0^2}{\epsilon_0} = C_\mu \frac{\chi^2}{\psi} \frac{\bar{U}_p A}{\theta_i A_i^{1/2}}$$

or the initial value of χ^2/ψ has an important effect on the turbulence intensity at TDC, u'_{TDC}. They varied χ^2/ψ from approximately 0.3 to 0.6. Figure 4 shows the results of varying χ^2/ψ over three orders of magnitude for $u_0' = 200$ cm/s. It shows the value of u' at the center of the computational domain, that is, at the half-radius of the chamber and midway

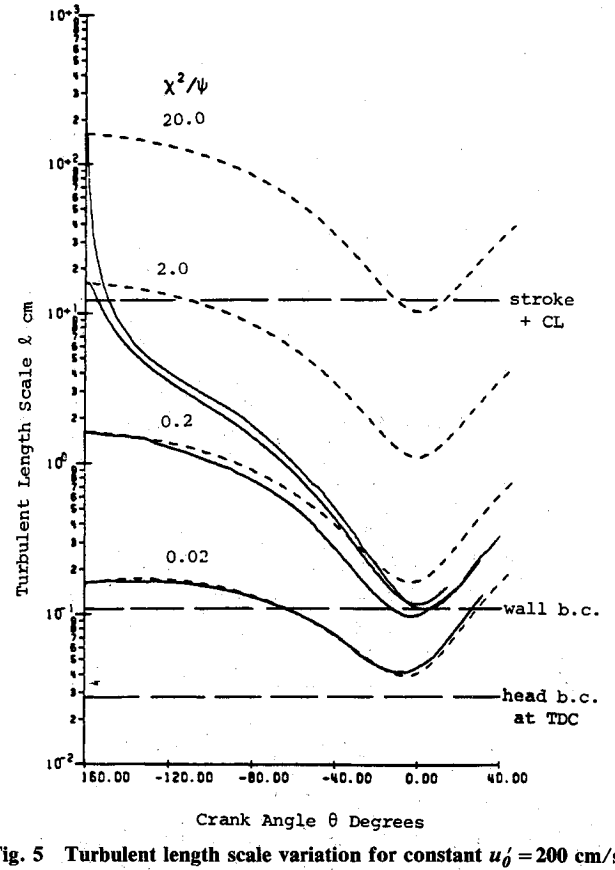

Fig. 5 Turbulent length scale variation for constant $u_0' = 200$ cm/s: ---- zero-dimensional model, —— two-dimensional model (ported engine, rpm = 2400, $\bar{U}_p = 914$ cm/s).

between the piston and the cylinder head. The results show that u'_{TDC} is sensitive to the initial value of χ^2/ψ for values around 0.2 and lower, but that for higher values of χ^2/ψ, u'_{TDC} is essentially independent of χ^2/ψ. Similar results for an order of magnitude higher $u'_0 = 2000$ cm/s are also shown in Fig. 4. The character of the results is the same. The initial turbulence level u'_0 has virtually no effect on u'_{TDC} for the same χ^2/ψ. The relaxation crankangle for the effects of the initial u'_0 to be forgotten is about 100-130 deg, in agreement with Grasso and Bracco.[21]

A qualitative explanation of these results can be offered. In the full two-dimensional model, there are two sources of production of turbulence—the axial compression and the shear at the cylinder walls due to piston motion. The initial turbulence in the engine due to intake processes is also being simultaneously dissipated. For high diffusivity, that is, large values of χ^2/ψ, the turbulence produced near the walls is rapidly diffused into the entire chamber and the maximum possible value of u' is attained in the central region of the engine chamber. For a fixed k_0 (or u'_0), the high initial value of χ^2/ψ also corresponds to a low initial value of ϵ (large initial length scale ℓ) and, therefore, the decay of turbulence is reduced in the early stages until the production of ϵ causes its buildup and leads to the decay of u' starting at around -30 deg. An examination of the behavior of the length scale ℓ as predicted by the model is quite interesting and the comparison of the results for ℓ obtained from the zero- and two-dimensional models is helpful in explaining the differences in the results. The results for the turbulent length scale ℓ for the zero- and two-dimensional models are presented in Fig. 5. For the two-dimensional model, for large χ^2/ψ, the initial ℓ is large. However, for large diffusivity the effect of the side-wall boundary condition on ℓ is also quickly felt across the engine chamber and causes a rapid decrease in the length scale ℓ. The length scales ℓ for the two largest values of χ^2/ψ become nearly identical and, with nearly the same values of u' as well, the development of u' and ℓ vs θ remains similar all the way to TDC. Thus, the two-dimensional model predicts a u' at TDC virtually independent of χ^2/ψ for values of $\chi^2/\psi > 0.2$. As Fig. 5 shows, for smaller $\chi^2/\psi \sim 0.02$, the ℓ remains small throughout the compression stroke and, due to the relatively higher dissipation rate, the u' at TDC is substantially lower. Figure 5 also explains the differences in the u' behavior between the zero- and two-dimensional solutions. In the zero-dimensional solution, there are no walls and therefore no wall boundary conditions on ℓ. The values of the length scale ℓ vs θ are quite different for different χ^2/ψ and consequently the u' values are also quite sensitive to the values of the diffusivity parameter χ^2/ψ.

The comparison of the two- and zero-dimensional results indicated the importance of the wall boundary condition. The length scale in the finite difference cell next to the wall is set at κy_p, where κ is a model constant (0.84) and y_p is the distance of the cell center from the wall. The sensitivity of the model results to the value of κ has been evaluated. As expected, a twofold increase in κ causes a significant change in length scale at the wall, but only a small effect ($<5\%$) on ℓ and u' in the middle of the engine chamber.

It is instructive to examine the relative magnitudes of the production (P^k) and the dissipation (ϵ) terms in the k equation for some of the parameters considered in the two-dimensional model calculations. Figure 6 shows the typical magnitudes of ϵ and the various components of P^k [Eq. (3)]. The specific results are for χ^2/ψ of 2.0 and $u'_0 = 200$ cm/s. The results support the earlier assertion in Sec. III that the $4/3\nu_T(\nabla \cdot \boldsymbol{u})^2$ part of the total production term is generally much smaller than $-2/3\, k \nabla \cdot \boldsymbol{u}$ in the complete two-dimensional solution of the equations. The important feature to note here is the fact that ϵ becomes the dominant term in the equation around $\theta = -30$ deg. As $\epsilon \sim k^{3/2}/\ell$ and ℓ is decreasing as θ is approaching TDC, this predicts a faster than exponential decrease of k and, given sufficient time, a value of k that is nearly independent of the starting value of k at around -30 deg, as shown in Fig. 4.

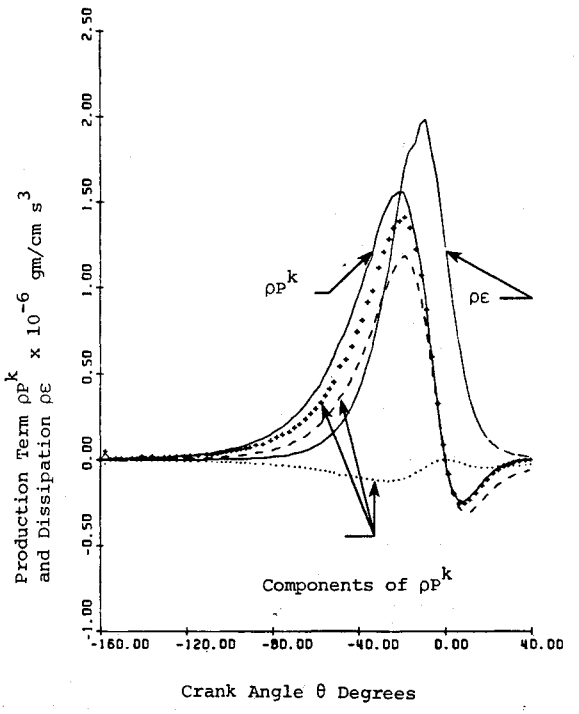

Fig. 6 Components of ρP^k and relative magnitudes of ρP^k and $\rho\epsilon$: —— total ρP^k and $\rho\epsilon$, + + + + $-2/3\,\rho k \nabla \cdot u + 4/3\mu_T(\nabla \cdot u)^2$, ---- $-2/3\,\rho k \nabla \cdot u$, · · · · $-2/3\,\mu_T(\Delta \cdot u)^2$ ($u'_0 = 200$ cm/s, $\chi^2/\psi = 2.0$, ported engine, rpm = 2400, $\bar{U}_p = 914$ cm/s).

This discussion leads to a number of important conclusions. First, the results of the simplified analyses agree with those of the full two-dimensional model for only a limited range of conditions, as was expected, that is, when the diffusion parameters are small so that the diffusive effects can be neglected. Thus, care has to be exercised in the general use of the zero-dimensional simplified analyses for predicting engine properties. Second, the two-dimensional model predicts a limit to the value of the turbulence intensity at TDC. The reason for the limit is the dominance of the turbulence dissipation ϵ in the k equation just prior to TDC due both to an increase in u' and a decrease in ℓ in turn imposed by compression and the walls.

Sensitivity of Results to Model Constants

An extensive study of the sensitivity of the calculated results to the model constants was carried out and is detailed in Ref. 16. A brief summary is presented here. The k-ϵ model involves six model constants. The value of $C_\mu = 0.09$ is quite standard, but somewhat different values of the other model constants have been used in other applications. We have explored broader ranges of the values of C_1, C_2, C_3, σ_k, and σ_ϵ than are usually considered to evaluate their effect on turbulence intensity at TDC.

The nominal values of each of the parameters and the range investigated in the sensitivity study are

C_1	*1.44*	*(1.0-2.0)*
C_2	*1.92*	*(1.5-2.5)*
C_3	*−1.0*	*(−3-+3)*
$\sigma_k, \sigma_\epsilon$	*1.0, 1.3*	*(0.5, 0.65-2.0, 2.6)*

Equation (7) shows that an increase of C_1 or a decrease of C_2 results in higher values of ϵ, which will lead to a faster decay of k. The trend of the results was as expected. A 30% decrease in C_1 leads to a 30% increase in u'_{TDC}, while a 39% increase in C_1 results in a 50% decrease in u'_{TDC}. The cor-

responding figures for C_2 are -22% change in C_2 leads to a -35% change in u'_{TDC}, while $+30\%$ change in C_2 results in $+15\%$ change in the turbulence intensity at TDC. C_3 brings in the effect of compressibility on the production of ϵ and was specifically added for IC engine problems[4,8,9] so that its value has not been extensively tested. Its effect can best be understood by considering an equation for ℓ, the turbulence length scale, that can be obtained by combining the equations of k and ϵ. For homogeneous turbulence, the equation for ℓ has the following form:

$$\frac{d\ell}{dt} = \frac{\ell}{k}\left[\left(\frac{3}{2} - C_1\right)P^k + \left(C_2 - \frac{3}{2}\right)\epsilon\right] - C_3(\nabla \cdot u)\ell$$

For large positive C_3, it is possible for ℓ to increase during the compression stroke when $\nabla \cdot u < 0$. Gosman and Johns[4] use a positive value of $C_3 = +1$, which does lead to an increase in ℓ in the initial phase of the compression stroke. We use $C_3 = -1$ to obtain a monotonic decrease of ℓ during compression. $C_3 = -3$ leads to large ϵ and very low u'_{TDC}. $C_3 = +3$ results in a 55% increase in u'_{TDC} compared to the results for our nominal value of -1.

The values σ_κ and σ_ϵ were simultaneously increased or decreased and the results are consistent with the corresponding decrease or increase in the diffusivity in the chamber. The u' at TDC was affected by about $\pm 30\%$.

Comparison with Measurements in a Ported Engine without Swirl

Grasso and Bracco[9] used the same two-dimensional model in comparisons with the data of Lancaster[2] in a valved engine and obtained satisfactory results for u' at TDC using an initial value of the diffusivity parameter $\alpha^2/\beta = 1.22$. The equivalent value of χ^2/ψ for the engine used by Lancaster is estimated to be between 0.6 and 0.7. The current series of comparisons with the data of Liou et al.[10,14,15] show that a value for $\chi^2/\psi = 0.5$ provides the best overall agreement. It is quite encouraging that essentially the same value of χ^2/ψ is capable of matching the data for two very different types of engines, that is, with ported or valved intakes.

Figure 7 shows the comparison of the model calculations with the data of Liou and Santavicca[14] at 1200 rpm in a ported engine without a swirl flow. The measurements were made at 12 different radial positions on 2 orthogonal diameters in the engine chamber at the center of the clearance height. The measurements at different positions define a band of data, the extent of which is represented by the two dotted lines in the figure. The computed turbulence intensity near TDC is at the low end of the range of data, but the decay rate of u' vs θ is in good agreement. Similar results are obtained at 1800 and 2400 rpm.

The actual flowfield in the ported engine at the end of the intake process is three-dimensional. The geometry of the intake ports results in a rolling motion of the intake flow inside the cylinder. This three-dimensional flow cannot be modeled with an axisymmetric model. To estimate its effect, which is expected to be an increase in u' due to the additional shears, computations were made in a planar engine configuration. The width of the engine was equal to the bore of the actual engine. The calculations simulate a rolling motion subject to compression in an rectangular duct of infinite length. A number of different roll velocity profiles were investigated and we concluded that the presence of the roll does generate a significant amount of turbulence in the early part of the compression stroke, but that near TDC the roll motion is virtually destroyed and there is only a small increase in TDC tur-

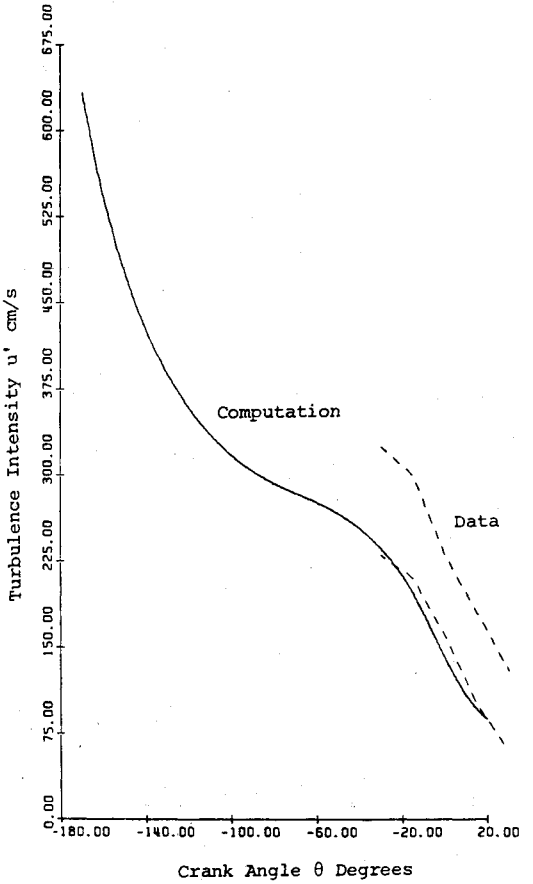

Fig. 7 Comparison of computed —— and measured range ---- of turbulence intensity ($u'_0 = 765$ cm/s, $\chi^2/\psi = 0.5$, ported engine, rpm = 1200, $\bar{U}_p = 457$ cm/s).

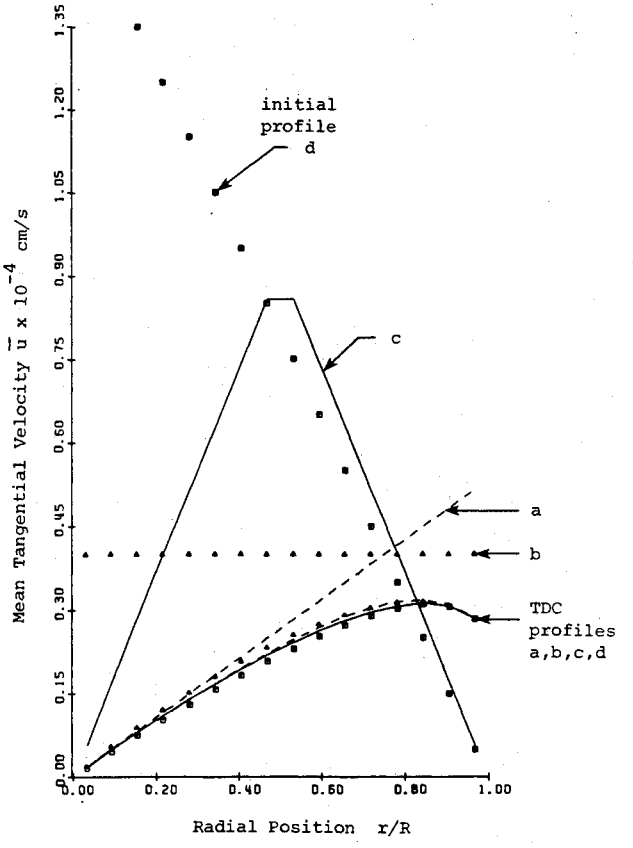

Fig. 8 Radial profiles of tangential velocity w—sensitivity of TDC profiles to four different initial profiles with the same angular momentum ($u'_0 = 1000$ cm/s, $\chi^2/\psi = 0.2$, ported engine, rpm = 2400, $\bar{U}_p = 914$ cm/s).

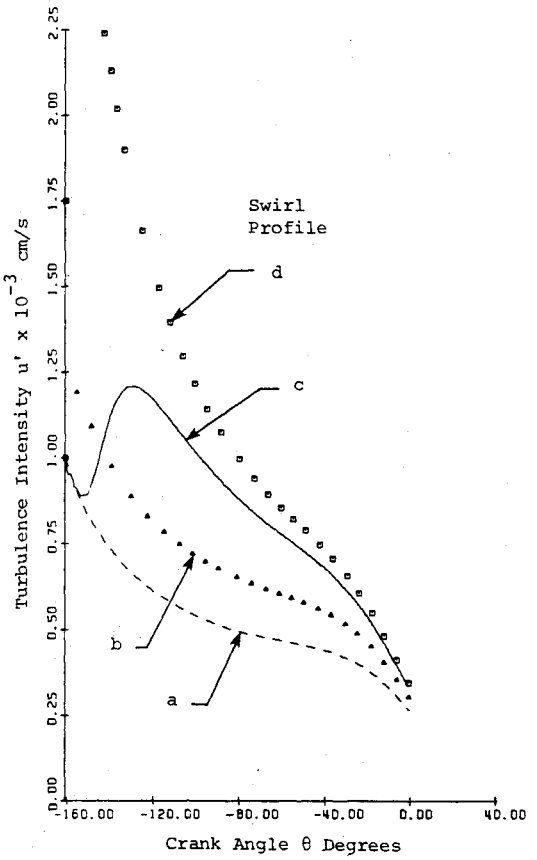

Fig. 9 Variation of turbulence intensity with crankangle for four different initial swirl profiles ($u'_\theta = 1000$ cm/s, $\chi^2/\psi = 0.2$, ported engine, rpm = 2400, $\bar{U}_p = 914$ cm/s).

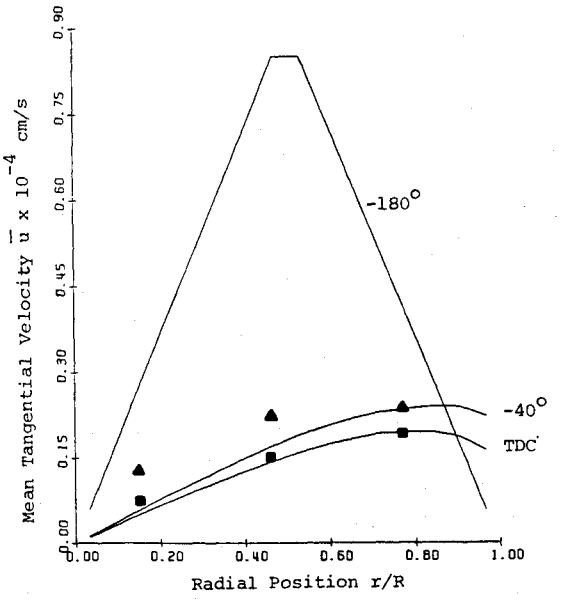

Fig. 10 Comparison of computed —— and measured (▲ −40 deg, ■ TDC) mean tangential velocity ($u'_\theta = 765$ cm/s, $\chi^2/\psi = 0.5$, ported engine, rpm = 1200, $\bar{U}_p = 457$ cm/s).

bulence.[16] Still, the presence of the rolling motion in the engine could lead to somewhat higher u' in the engine near TDC and improve the agreement with experimental data, but a three-dimensional calculation is necessary to verify this supposition.

Analysis of Swirl Velocity Fields

Liou and Santavicca[14] also made measurements in the ported engine of Fig. 1 with swirl at three different engine speeds. Measurements of the mean tangential velocity w were made from −40 to +20 deg crankangles. However, there is no information on the initial w velocity profile existing at the time of inlet port closure. The sensitivity of the model to four different initial swirl profiles with the same total angular momentum was examined. Figure 8 shows the four initial mean w velocity profiles at −160 deg and the resulting profiles at TDC. In all cases, the TDC swirl velocity profile is essentially a solid-body rotation matched to a wall boundary layer, which is in agreement with the results of El Tahry.[6] The four quite different initial swirl profiles lead to essentially the same swirl velocity profile at TDC, that is, the decay of the swirl angular momentum is nearly the same for all these profiles. The adjustment to this equilibrium profile is quite rapid and takes place in 20-30 deg crankangles. Due to the very different mean shear in the four initial profiles, the development of u' with θ is quite different, as shown in Fig. 9, but by TDC u' is virtually independent of the initial swirl velocity profile. The figure shows the u' values in the middle of the engine chamber. For solid-body rotation (profile a), there is no production of turbulence due to mean shear in the swirl velocity and u' simply decays from the beginning. For profiles c and d, which have high shear, u' may increase by significant amounts for initial crankangles. Nonuniform shear in the swirl profile (such as profile c) leads to an initially quite nonuniform radial u' profile in the chamber, but by TDC the turbulence is essentially homogeneous in the engine chamber.

Comparison with Measurements in Ported Engine with Swirl

The model predictions at 1200 rpm for w and u' using the initial diffusivity parameter $\chi^2/\psi = 0.5$ are shown in Figs. 10 and 11. As discussed in the previous section, the results at TDC are independent of the initial swirl velocity profile and depend only on the initial total angular momentum. A triangular initial w profile (profile c of Fig. 8) was used in the calculations. The initial value of w_{max} was selected by trial and error to match the measured total angular momentum at TDC. The measured w profile across the engine is not completely symmetrical and the average values of the two sides are used in the figure. The measured w profile at −40 deg shows more of a "top-hat" nature than is seen in the calculated profile. The calculated w profile at TDC is in good agreement with the data. The range of measured u' at six different radial positions across the chamber is plotted in Fig. 11 as a pair of dotted lines. The model predictions at three radial positions are compared to the experimental data. The computed u'_{TDC} is about 30% lower than the measured value and the u' vs θ decay rate is somewhat different.

Improving the agreement with data is difficult as the model results for the swirl flow case show even less sensitivity than the no-swirl case to changes in the diffusivity parameter χ^2/ψ or initial u', consistent with the results of Grasso and Bracco.[21] The three-dimensionality of the flowfield could be partly responsible for the disagreement in the magnitude and slope of u', but this can be ascertained only from an unsteady three-dimensional computation.

Comparison with Measurements in a Valved Engine without Swirl

The comparison of the model predictions with the experimental measurements for the valved engine led to a rather satisfying demonstration of the promise of modeling and of the advantages of iterative combinations of experiments and computations. Liou[22] made turbulence measurements also in a valved engine to study the possible effects of different intake systems. The measurements were made from −40 to +20 deg in a four-stroke, four-valve engine with a pancake combustion chamber without swirl. The dimensions and operating parameters of the valved engine are quite similar to those of

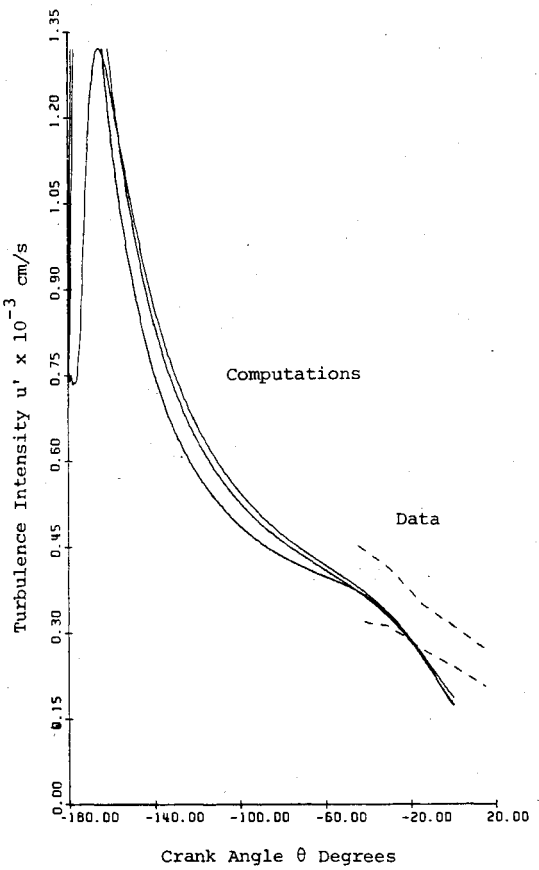

Fig. 11 Comparison of computed —— and measured range ---- of turbulence intensity; the three solid lines represent three different radial positions in the midplane of the chamber ($u_0' = 765$ cm/s, $\chi^2/\psi = 0.5$, ported engine, rpm = 1200, $\bar{U}_p = 457$ cm/s).

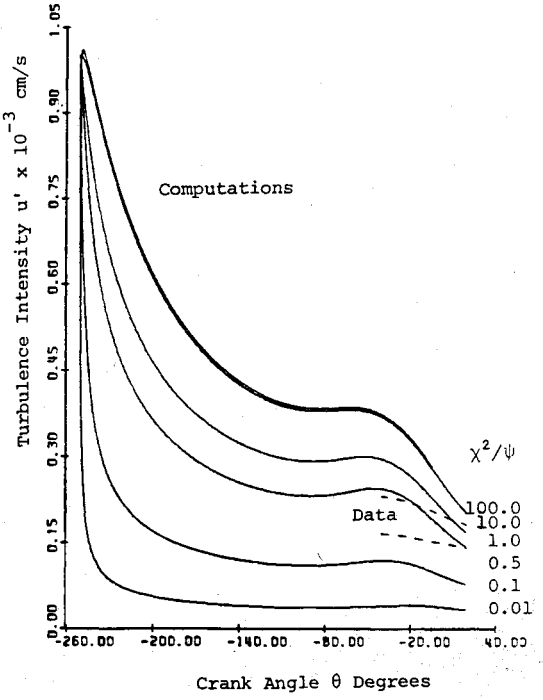

Fig. 12 Comparison of computed —— and measured range ---- of turbulence intensity ($u_0' = 1000$ cm/s, valved engine, rpm = 1800, $\bar{U}_p = 686$ cm/s).

the ported engine (see Fig. 1). The initial measurements[22] indicated a TDC turbulence intensity that was approximately five times higher than that measured in the ported engine for the same engine speed. The high values of u'_{TDC} were quite surprising, since they were higher than any other reported data for pancake-type simple combustion chambers without either swirl or squish. Also, the model, which had been quite successful in many previous comparisons with experimental data for different engines, could not come anywhere close to those measured u'_{TDC} values. The model sensitivity studies described in Sec. IV showed that the u'_{TDC} does not increase by more than 50%, even with extreme changes in one model constant at a time. It is unlikely that even a combination of changes in the model constants would cause a fivefold increase in u'_{TDC}. The exercise of the model led us to the conclusion that the measurements must be erroneous. The measurements in the valved engine were then repeated[15] and the revised data indicated turbulence levels near TDC very similar to those in the ported engine without swirl. The predictions for the valved engine are compared to the measurements in Fig. 12. The calculations were initialized using $u_0' = 1000$ cm/s at -251 deg and χ^2/ψ values of 0.01-100.0. For $\chi^2/\psi = 0.5$ (the same value that was used in the ported engine comparisons), the model predictions are in good agreement with the measurements. The u' vs θ decay in the calculations is somewhat faster than the measurements.

V. Conclusions

As reported by Grasso and Bracco,[9] the intensity of turbulence near TDC in engines with pancake chambers (i.e., without squish) increases when the diffusivity of the turbulence generated by the intake process increases.

However, after a point, further increases in initial diffusivity produce smaller and smaller increases in TDC turbulence intensity. Thus, there is a practical limit to the maximum value of the TDC turbulence intensity that can be reached in such engines. Computations and measurements[15] indicate that the maximum value of the TDC turbulence intensity is about one-half the mean piston speed ($u'_{TDC} \leq \bar{U}_p/2$) when the intensity of turbulence is defined as the intensity of the high-frequency components of the velocity fluctuations in cycle-resolved measurements,[10,14,15] which we believe is the correct definition for combustion studies.

The limit was found through the computations reported in this paper when higher values of the initial diffusivity than those explored by Grasso and Bracco[9] were investigated. It is due to the chamber walls. The higher is the turbulence diffusivity generated by the intake process, the sooner is the turbulence damping effect of the walls felt all the way to the center of the chamber. In addition, we made the following findings.

With the use of the same model parameters as in previous studies[9] and an initial diffusivity parameter $\chi^2/\psi = 0.5$, the computed magnitudes of the turbulence intensity near TDC agree well with the measurements of Liou et al.[10,14,15] for a ported engine with and without swirl and also a valved engine. There is some disagreement in the rate of decay of the turbulence intensity near TDC; but, considering the current state of the knowledge of turbulence in general and engine turbulence in particular, as well as experimental uncertainties, the level of agreement between the computed and measured values can be considered acceptable.

The actual flowfield in the ported engine is three-dimensional due to a roll motion produced by the intake. A three-dimensional computation that includes the roll motion may also lead to better agreement between computed and measured quantities.

Also, as shown by the sensitivity studies, the agreement could be improved by changes in the k-ϵ model constants. However, this is not a recommended procedure as the identical set of model constants has been successfully used in several different turbulence problems, including previous internal combustion engine studies. A change in constants would require a reconsideration of previous applications and it is unlikely that an overall improvement would result.

As previously shown by Grasso and Bracco,[9,21] model predictions near TDC are insensitive to the initial turbulence intensity (depending only on the initial turbulence diffusivity) and the relaxation crankangle is of the order of 100-130 deg.

For swirling flows, the predicted mean tangential velocity profile at TDC is essentially a solid-body rotation plus a wall boundary layer and is independent of initial inlet profile. The predictions for swirl velocity are in reasonable agreement with the limited data presently available.

There are substantial disagreements between the solutions of the k-ϵ equations under certain commonly made simplifying assumptions and the solution of the full motion equations. Thus, although simplified analyses can be instructive, considerable care has to be exercised in their use.

Acknowledgments

Support for this work was provided by the U.S. Department of Energy (Contract DE-AC-04-81AL16338), the National Science Foundation (Grant CPE80-03483), and Cummins Engine. Some of the results were presented at the 18th Direct Injection Stratified Charge Engine (DISC) Meeting, Princeton University, September 1983 and at the 19th DISC Meeting, General Motors Research Laboratories, March 1984.

References

[1]Semenov, E.S., "Studies of Turbulent Flows in Piston Engines," NASA TTF-97, 1963.

[2]Lancaster, D.R., "Effects of Engine Variables on Turbulence in A Spark-Ignition Engine," SAE Paper 760159, 1976.

[3]Witze, P.O., "Measurements of the Spatial Distribution and Engine Speed Dependence of Turbulent Air Motion in an I.C. Engine," SAE Paper 770220, 1977.

[4]Gosman, A.D. and Johns, R.J.R., "Development of a Predictive Tool for In-Cylinder Gas Motion in Engines," SAE Paper 780315, 1978.

[5]Ramos, J.I., Humphrey, J.A.C., and Sirignano, W.A., "Numerical Prediction of Axisymmetric Laminar and Turbulent Flows in Motored, Reciprocating Internal Combustion Engines," SAE Paper 790356, 1979.

[6]El Tahry, S.H., "A Numerical Study of the Effects of Fluid Motion at Inlet-Value Closure on Subsequent Fluid Motion in a Motored Engine," SAE Paper 820035, 1982.

[7]Syed, S.A. and Bracco, F.V., "Further Comparisons of Computed and Measured Divided-Chamber Engine Combustion," SAE Paper 790247, 1979.

[8]Morel, T. and Mansour, N.N., "Modeling of Turbulence in Internal Combustion Engines," SAE Paper 820040, 1982.

[9]Grasso, F. and Bracco, F.V., "Computed and Measured Turbulence in Axisymmetric Reciprocating Engines," *AIAA Journal*, Vol. 21, April 1983, pp. 601-607.

[10]Liou, T.M., Santavicca, D.A., and Bracco, F.V., "Turbulence Measurements in a Ported IC Engine," Paper presented at International Symposium on Applications of Laser-Doppler Anemometry to Fluid Mechanics, Lisbon, 1982.

[11]Dent, J.C. and Salama, N.S., "The Measurement of the Turbulent Characteristics in an Internal Combustion Engine Cylinder," SAE Paper 750886, 1975.

[12]Johnston, S.C., Robinson, C.W., Rorke, W.S., Smith, J.R., and Witze, P.O., "Application of Laser Diagnostics to an Injected Engine," SAE Paper 790092, 1979 (see also Sandia National Laboratories, Albuquerque, N. Mex., Rept. SAND81-8242, 1981).

[13]Rask, R.B., "Laser Doppler Anemometer Measurements in an Internal Combustion Engine," SAE Paper 790094, 1979.

[14]Liou, T.M. and Santavicca, D.A., "Cycle Resolved Turbulence Measurements in a Ported Engine with and without Swirl," SAE Paper 830419, 1983.

[15]Liou, T.M., Hall, M., Santavicca, D.A., and Bracco, F.V., "Laser Doppler Velocimetry Measurements in Valved and Ported Engines," SAE Paper 840375, 1984.

[16]Hayder, M.E., Varma, A.K., and Bracco, F.V., "A Limit to TDC Turbulence Intensity in Internal Combusion Engines," Mechanical and Aerospace Engineering Dept., Princeton University, Princeton, N.J., Rept. 1667- MAE, June 1984.

[17]Borgnakke, C., Davis, G.C., and Tabaczynski, R.J., "Predictions of In-Cylinder Swirl Velocity and Turbulence Intensity for an Open Chamber, Cup in Piston Engine," SAE Paper 810224, 1981.

[18]Tabaczynski, R.J., "Turbulence Measurements and Modeling in Reciprocating Engines—An Overview," *International Conference in Engineering*, Vol. I, I.Mech.E. Conference Publications 1983-3, Mechanical Engineering Publications Ltd., London, 1983, pp. 51-64.

[19]Reynolds, W.C., "Modeling of Fluid Motions in Engines: An Introductory Overview," *Combustion Modeling in Reciprocating Engines*, edited by J.N. Mattavi and C.A. Amann,Plenum Press, New York, 1980, pp. 41-68.

[20]Davis, G.C. Tabaczynski, R.J., and Belaire, R.C., "The Effect of Intake Valve Lift on Turbulence Intensity and Burnrate in S.I. Engines—Model versus Experimental," SAE Paper 840030, 1984.

[21]Grasso, F. and Bracco, F.V., "Sensitivity of Chamber Turbulence to Intake Flows in Axisymmetric Reciprocating Engines," *AIAA Journal*, Vol. 21, April 1983, pp. 637-640.

[22]Liou, T., "Laser Doppler Velocimetry Measurements in Valved and Ported Engines," Ph.D. Thesis No. 1602-T, Dept. of Mechanical and Aerospace Engineering, Princeton University, Princeton, N.J., May 1983.